Histol Histopathol (2015) 30: 1203-1211

http://www.hh.um.es

Histology and Histopathology

Cellular and Molecular Biology

Inter- and intra-tumoral relationships between vasculature characteristics, GLUT1 and budding in colorectal carcinoma

Artur Mezheyeuski[1,2], Alexander Nerovnya[2], Tatjana Bich[2], Gennadiy Tur[3], Arne Ostman[1] and Anna Portyanko[2]

[1]Department of Oncology- Pathology, Karolinska Institutet, Stockholm, Sweden, [2]Department of Pathology, Belarusian State Medical University, Minsk, Belarus and [3]Minsk City Clinical Oncology Dispensary, Minsk, Belarus

Summary. Vascular characteristics, hypoxia and tumor budding are features that have been implied in the biology and prognosis of colorectal cancer. Internal relationships and the inter- and intra-tumoral variation of these tumor properties remain to be determined. In the current study we have characterized blood vessel status in different areas of CRC and in the peritumoral fibroblastic stroma. Analyses of these characteristics have been supplemented by characterization of budding and hypoxia.

Analyses revealed significantly lower values of vessel perimeter (VP) and vessel lumen area (VL) at the invasive front and surrounding stroma as compared to the tumor center. Also, the number of vessels (VN) in the peritumoral stroma was higher than in the center. Thus, tumor center displays larger and fewer vessels as compared to the tumor periphery.

GLUT1 expression was correlated directly with VN (r=0.351, p=0.028) and inversely with VL and VP (r=-0.432, p=0.006 and r=-0.484, p=0.002) at the invasive front. Moreover, GLUT1 expression, VP at the invasive front, and VN in the surrounding peritumoral stroma, were associated with budding score (r=0.574, p<0.000, r=-0.340, p=0,034 and r=-0,389, p=0.025 respectively).

Furthermore, GLUT1, budding score, vessel number in peritumoral stroma, and vessel size in the invasive front, were significantly different in tumors with or without lymph node metastasis.

This study reports previously unrecognized relationships between localization-specific vascular characteristics, hypoxia and tumor budding. The findings suggest potential functional relationships, which should be further explored, and also highlight the inter-tumoral variations in vasculature, which is highly relevant for ongoing efforts to identify vessel-based biomarkers.

Key words: Colorectal cancer, Vessel density, Budding, GLUT1

Offprint requests to: Mezheyeuski Artur, Cancer Center Karolinska, R8:03, Department of Oncology- Pathology, Karolinska Institutet, Stockholm, SE-171 76, Sweden, e-mail: artur.mezh@gmail.com

DOI:10.14670/HH-11-613

Introduction

Colorectal cancer (CRC) is one of the most common malignant diseases in Europe and the third leading tumor in the world (Ferlay et al., 2010). The most common reason of death in cancer patients is metastases formation. Tumor vasculature and vessel wall characteristics are assumed to be linked to cancer cell intravasation and distant metastases development (Bockhorn et al., 2007). Tumor growth involves active modification of pre-existing tissue. During this process the stromal cells will alter the phenotype, invasiveness and metastatic capacity of carcinomas.

Neovascularization is an essential stroma-related factor for tumor progression. It is accepted that a tumor is not able to exceed a volume of 1-2 mm^3, without induction of new vessel formation (Mosch et al., 2010). Tumor vessels develop in response to angiogenic chemokines, produced by both stromal and cancer cells

(Carmeliet and Jain, 2011). Cancer-associated vasculature and vessel wall characteristics are related not only to primary tumor growth, but also to cancer cell intravasation and establishment of distant metastases (Bockhorn et al., 2007). Determining the status and nature of tumor vasculature in human tissue involves evaluation of the expression of endothelial cell markers. However, commonly used markers CD31, CD34, CD105 and von Willebrand factor are not equivalent. Their expression may differ depending on vessel status and differentiation grade (Yao et al., 2007).

New vessel formation is affected by stroma oxygenation and metabolism status (Fraisl et al., 2009). Hypoxia has been reported as an important characteristic of solid tumors linked to angiogenesis, glycolytic metabolism and overall survival (Dachs and Tozer, 2000). Hypoxic conditions are also considered as a driving force in establishment of metastatic phenotype (Sullivan and Graham, 2007). A key regulator of cell adaptation to hypoxic conditions is hypoxia inducible factor-1a (Hif-1a), which controls expression of factors such as vascular endothelial growth factor (VEGF), carbonic anhydrase-9 (CA-IX), lactate dehydrogenase-A (LDH-A) and facilitative glucose transporter-1 (GLUT-1) (Quintero et al., 2004). Increased glycolysis is one of the adaptation mechanisms for cancer cells in hypoxic conditions (Gatenby and Gillies, 2004). To be able to consume glucose, the cell needs to transport it into the cytosol. GLUT1, the integral membrane glycoprotein, is one of the major proteins responsible for glucose uptake in most normal and cancer cells (Asano et al., 1991).

Tumor budding is defined as the presence of single cells or cell clusters (up to 5 cells) disseminated in the stroma at the invasive front of the tumor (Jass et al., 2003). Budding has been reported to be one of the major prognostic characteristics in CRC and has been linked to epithelial–mesenchymal transition. Pan-cytokeratin staining facilitates accurate scoring of tumor buds. However, different counting methods have been developed and applied to evaluate the intensity of tumor budding (reviewed in Mitrovic et al., 2012; Horcic et al., 2013).

Microvessel density (MVD) is a parameter frequently used to quantify vessel status in cancer tissue. However, MVD is not correlated with sufficient blood supply (Zhang et al., 2009). There is also conflicting data indicating presence or absence of the linkage between MVD and perfusion parameters, measured preoperatively by computed tomography. Although MVD was reported to be associated with blood flow in some of the publications, no such correlation was found between MVD and glucose uptake in CRC (Goh et al., 2008, 2012). One can hypothesize that tissue oxygen/glucose supply is dependent not on total vessel number, but rather on mature, normally functioning vessels, having adequate blood/tissue interaction area. Another issue to consider regarding analyses of MVD is the tumor region to be analyzed. MVD is most commonly evaluated in the center of the tumor or in so-called hot-spots. However, based on the potential importance of the invasive region for metastasis it can be argued that the functional significance of MVD in this area is of equal, or even greater functional importance. This notion is supported by earlier preliminary studies, which have demonstrated differences in vessel characteristics between different tumor areas (Vlems et al., 2004; Rajaganeshan et al., 2007), and studies which have noted hyperexpression of hypoxia markers (Hif-1a, GLUT1, CA-9) at the invasive margin of CRC (Rajaganeshan et al., 2009).

In the current study we have characterized blood vessel status in different areas of CRC and in the peritumoral fibroblastic stroma. Analyses of these characteristics have been supplemented by analyses of budding and hypoxia, to explore potential associations between vessel characteristics, hypoxia and budding.

Materials and methods

This study was approved by the Ethic Committee of Belarusian State Medical University.

The study was performed on 39 surgically resected

Table 1. Patients' cohort characterization.

Characteristics		Number of cases (%)[a]
Age mean (y); range		63,64; 44-84
Gender	Male	11 (28)
	Female	28 (72)
Localization	Caecum	5 (13)
	Ascending	3 (8)
	Transverse	1 (3)
	Descending	4 (10)
	Sigmoid	15 (38)
	Rectum	11 (28)
Stage	I	5 (13)
	II	9 (23)
	III	17 (44)
	IV	8 (21)
Differentiation grade	Well/moderate 33 (85)	
	Poor/undifferentiated 6 (15)	
Extent of invasion	Submucosa (T1)	0 (0)
	Muscularis propria (T2)	5 (13)
	Perirectal tissue and pericolic (T3)	27 (69)
	Adjacent structures (T4)	7 (18)
Lymph node status	Intact	13 (33)
	Lymph node metastases	26 (67)
Number of lymph nodes collected, median (mean; range)		19 (17,97; 1-51)
Presence of distant metastases		8 (21)

[a] in some cases mean and range are indicated instead of number and percentage.

non-mucous colorectal carcinomas. Clinicopathologic and demographic characterization of the cases are summarized in Table 1. One surgeon operated all tumors. No neoadjuvant treatment was applied. Resected tissue was fixed in 10% formalin for 48 hours. Then, samples were transverse sliced, blocks from tumor center and the invasive area were cut out, dehydrated and paraffin embedded. Lymph node evaluation procedure followed principal (UICC/AJCC) rules. After routine histological evaluation sections of deepest invasion were selected.

Immunohistochemistry and immunofluorescence

4 μm thick sections were cut from the tissue blocks and mounted on slides. Sections were then deparaffinized in xylene and rehydrated in ethanol. Antigen retrieval was carried out using citrate buffer (pH 6.0) for GLUT1 (clone SPM498, Abcam, Cambridge, UK) and Tris-EDTA buffer (pH 9.0) for cytokeratin (clone AE1/AE3, Dako, CA, USA) and CD34 (clone JC70A, Dako, CA, USA) in Pascal Pressure Cooker (Dako, CA, USA) (1250C, 30 sec for GLUT1 and CD34 and 1250C, 2,5 min for cytokeratin). Endogenous peroxidase was blocked with 3% H_2O_2 (20 min) and nonspecific binding was eliminated by 30 min of incubation with 10 g/L bovine serum albumin in Tris-buffered saline. The sections were incubated at +40C overnight with a monoclonal mouse anti-CD34, and monoclonal mouse anti-GLUT-1 at the dilution of 1:100 and 1:200 respectively, followed by incubation with the amplification system (EnVision + System-HRP Dako A/S, EnVisionTM, Dako, CA, USA) for 30 min at room temperature. Diaminobenzidine (DAB) detection system was used for specific staining and hematoxylin as counterstain.

For budding detection anti-cytokeratin antibody (clone AE1/AE3, IgG1-isotype, Dako, CA, USA) at the dilution 1:400 was used. Secondary antibodies Alexa Fluor® 488 Goat Anti-Mouse IgG1 (Life Technologies, OR, USA) were applied at 1:200 dilution for 2 h at room temperature. Counterstaining of nuclei was performed by 4',6-diamidino-2-phenylindole, dihydrochloride (DAPI) (Sigma, MO, USA). All slides were mounted in Fluorescence Mounting Medium (Dako, CA, USA). For negative control the same procedure was applied with Isotype Control For Mouse Primary Ab (Life Technologies, OR, USA).

CD34 staining evaluation

All specimens were examined using a Leica DM5000B microscope with HC PL FLUOTAR objectives. Sections were scanned at low magnification and representative areas at tumor center, invasive front and peritumoral stroma were selected. The regions with prominent inflammation, necrosis, hemorrhage, or cyst formation were avoided. Images were acquired at ×20 using a DFC420C Leica digital camera (2592×1944 pixels). The invasive margin was determined as the border between malignant cell clusters and peritumoral stroma. The regions adjacent to this border from the tumor side were considered as "invasive front area". The regions adjacent to invasive margin from stromal side were considered as "peritumoral stroma area". The entire invasive front area was captured resulting in an average of 10 (6-13) images per slide. When making photos from central parts of the tumor three cases were excluded because of the absence of appropriate tissue in this area. In the peritumoral area only fibroblastic stroma was selected: muscle tissue (for T2 stage tumors) and fat tissue was excluded (6 cases) for such analysis. An average of 9 and 8 photos per case were made for central and peritumoral area respectively.

Color deconvolution technique provides the possibility to separate immunohistochemical staining by means of color image (Ruifrok et al., 2003). For the study Color Deconvolution algorithm for DAB (for locating the antigen of interest) and hematoxylin (counterstain) was implemented as an NIH-ImageJ (http://rsb.info.nih.gov/ij/) plugin (Ruifrok and Johnston's algorithm (Ruifrok and Johnston, 2001)). The plugin processes a primary RGB image and creates three 8-bit monochrome images. One of them representing DAB stain was used for future analysis. Every 8-bit DAB-related image was converted into "binary" black-and-white, thus converting CD34-marked-DAB-stained vessels into black particles. Particle Analysis plugin was applied after that (http://www.uhnresearch.ca/facilities/wcif/imagej/particle_analysis.htm.). Particle (vessel) number, perimeter (measured in pixels) and surface area (measured in square pixels) were traced. Mean values of Vessel Number, Vessel Perimeter and Vessel Lumen per each tumor region were calculated for each case.

GLUT-1 staining evaluation

It was shown in previous studies that GLUT1 expression may differ between different areas (central vs periphery) of CRC tumor (Rajaganeshan et al., 2009). In the present study we focus on the marker profile at the invasive front area.

DAB-based staining has been shown to be sufficient to estimate the amount of an antigen present in an immunohistochemically stained section (Matkowskyj et al., 2003; Taylor and Levenson, 2006; Krajewska et al., 2009). Two different types of metrics were obtained in our study: Positivity, which only characterizes quantity of positive stained pixels, and average Optical density (OD), which represents the intensity of positive pixels. For quantification and data presentation we use the combined value (Rizzardi et al., 2012): Product (Positivity x OD).

Images were acquired at ×20 using a DFC420C Leica digital camera (2592×1944 pixels). Three images

per case from the invasive area were made. The images were then processed to generate signal-mask pairs, using Photoshop CS3 (Adobe, San Jose, CA, USA). Areas of pure tumor tissues with no stroma, necrosis, hemorrhage, or cyst formation were selected. The size of the selected areas was traced in pixels. The obtained images were then analyzed by the image analysis software, ImageScope v. 11.1.2.752 (Aperio Technologies, Inc.). The Positive Pixel Count Algorithm v.9 was used for quantitative evaluation of IHC (Krajewska et al., 2009; Portyanko et al., 2009). The thresholds for weak, medium and strong intensity of staining were set as default. GLUT1 staining was considered as "positive". The following parameters were used in the study: Nwp, Np and Nsp – number of weak positive, moderate positive and strong positive pixels respectively; Iwp, Ip and Isp – total intensity of weak positive, moderate positive and strong positive respectively; NxpT = Nwp+Np+Nsp – total number of positive pixels; Iavg = (Iwp+Ip+Isp)/(Nwp+Np+Nsp) – average intensity of positive pixels.

According to the Positive Pixel Count Algorithm v.9 User Guide "intensity" is the measure of brightness of the pixel, which is proportional to the amount of light transmitted through the slide. Stained tissue blocks the light and thus is reciprocal to the intensity, so optical density value had to be calculated (Beer–Lambert law):
OD = -log(Iavg/I0) = average optical density of positive pixels
Then Positivity and Product values were calculated:
Positivity = NxpT/TN
Product = Positivity x OD
where TN is total selected area size in pixels traced previously for every image; I0 is intensity of light if no object was in the light path (Krajewska et al., 2009), and was set as 220 in the Scan Scope. Obtained Product value was used for further analysis.

Budding evaluation

Tumor buds are single cancer cells or cell clusters composed of up to 5 cells, disseminated from the invasive margin. To facilitate cancer cell recognition, the majority of the budding scoring systems utilize immunostained samples (Horcic et al., 2013). In the present study we used immunofluorescence (IF) as a visualization technique. This was used together with cell nuclei staining to facilitate a more accurate and robust distinction between buds and bigger cell clusters.

Images were obtained on automated Leica DM5000 B microscope with automated fluorescence axis using a Leica DFC420 C digital camera. For DAPI and cytokeratin signals A4 and L5 filtercubes (Leica Microsystems, Wetzlar, Germany) were used respectively. For each case 10 consecutive non-overlapping fields from the deepest part of invasive front for each channel were acquired under ×200 magnification. Total number of tumor budding foci was counted in each field. Only clusters containing 5 or less nuclei were considered to be a tumor budding foci. Mean number of tumor budding per field was calculated for each case.

Statistical analysis

Associations between GLUT1 expression, grade of budding and vessel characteristics were analyzed by Spearman rank correlation test. The difference between groups was assessed using Mann–Whitney U-test. Two-tailed p-values of <0.05 were considered as statistically significant. All statistical analyses were carried out using SPSS V20 (SPSS Inc., Chicago, IL)

Results

The vasculature of the invasive front and the peritumoral stroma show different and independent characteristics as compared to the vasculature of the tumor center

To characterize the internal vascular heterogeneity in CRC, vascular characteristics were analyzed separately in the center of the tumor, at the invasive front and in the peritumoral fibroblastic stroma (Fig. 1A). In each region number of vessels (VN), mean vessel perimeter (VP) and mean vessel lumen area (VL) were determined.

Evaluation of vessel characteristics revealed significantly lower values of VP and VL at the invasive front and surrounding stroma as compared to the tumor center. Also, VN in peritumoral stroma was higher than in the center (Fig. 1B). Thus, the tumor center displays larger and fewer vessels as compared to the tumor periphery.

The next analysis aimed at investigating potential correlations between vascular characteristics in the different regions within the individual patients. According to this analysis vessel metrics of peritumoral stroma was not correlated to the characteristics of the tumor vasculature (data not shown). The only significant correlation observed in this analysis was the positive correlation between vessel number in the central part of the tumor and at the invasive front (Fig. 2).

Together these analyses demonstrate consistent differences between the vascular characteristics of the

Table 2. GLUT1 expression and vessel characteristics associations at the invasive front.

The invasive front vessel characteristics	GLUT1 (n=39)	
	correlation coefficient	p value
vessel number	0.351	0.028
lumen area	-0.432	0.006
perimeter	-0.484	0.002

n, number of cases.

central part of the tumor and the invasive front and peritumoral stroma.

Vessel density, vessel perimeter and lumen area at the invasive front, are associated with GLUT1 expression

Microvessel status controls oxygen and glucose supply, and is also regulated by these features. GLUT1 is a glucose transporter, and previous studies have linked GLUT1 expression to hypoxia and hypoglycemia. GLUT1 expression was therefore analyzed and correlated with vascular characteristics in our study.

In agreement with the previous reports, differential expression of GLUT1 at the invasive front was observed when different tumor samples were compared (Fig. 3).

When analyzed by Spearman rank correlation, all vessel characteristics of the invasive front were found to be significantly associated with the level of GLUT1 (Table 2). The highest GLUT1 expression was observed in the tumors with the highest number of small vessels at the invasive front. In contrast, GLUT1 expression at the

Table 3. Grade of budding associations with GLUT1 expression at the invasive front and vessel characteristics in different tumor areas.

Region and characteristics analyzed		budding	
		correlation coefficient	p value
C (n=36)	VN	-0.187	0.274
	VL	0.073	0.674
	VP	-0.084	0.628
I (n=39)	VN	0.252	0.122
	VL	-0.211	0.197
	VP	-0.340	0.034
S (n=33)	VN	-0.389	0.025
	VL	0.188	0.295
	VP	0.143	0.428
GLUT1 (n=39)		0.574	<0.000

VN, number of vessels; VL, vessel lumen; VP, vessel perimeter; C, central area; I, invasive front; S, peritumoral fibroblastic stroma; n, number of cases; p, p-value.

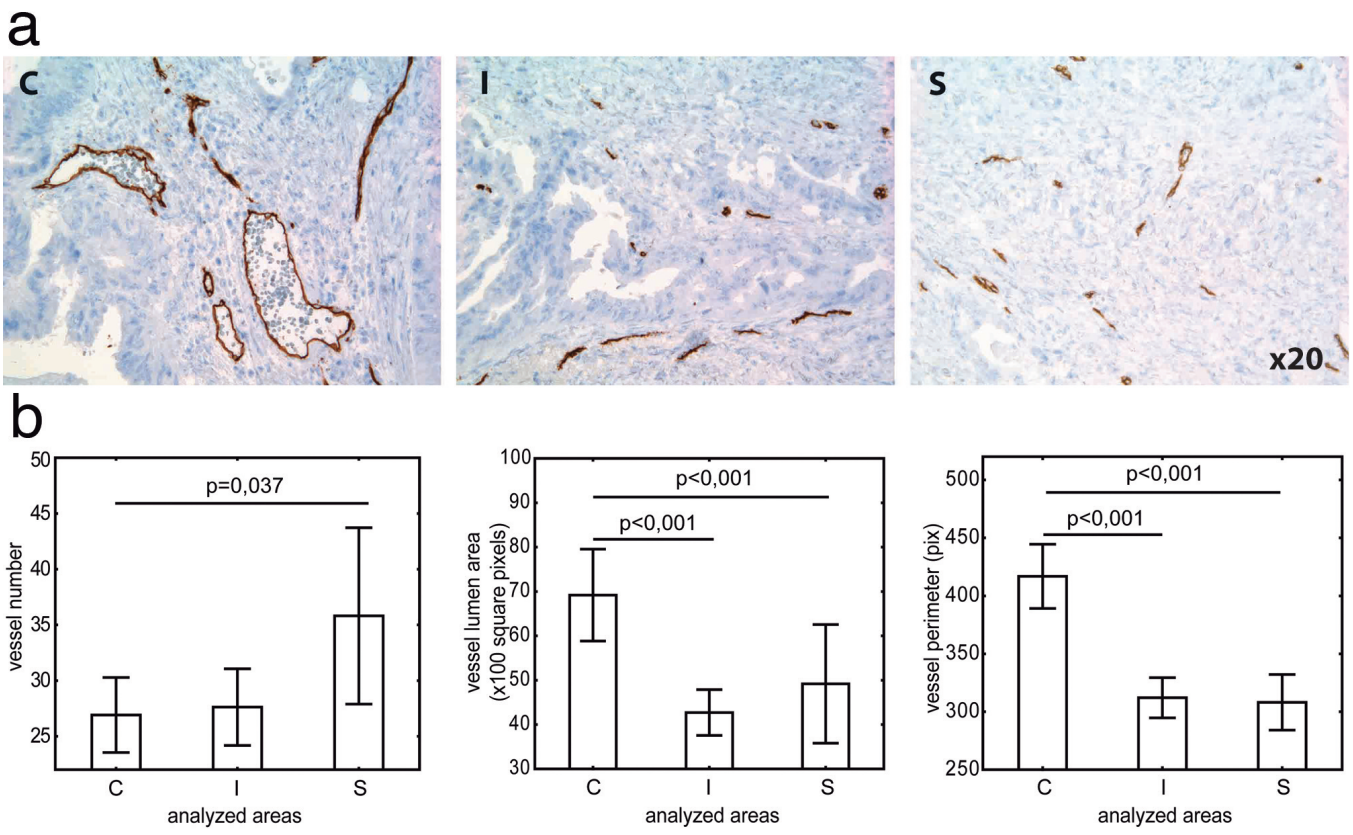

Fig. 1. Vasculature characteristics differ between central tumor area and invasive or peritumoral area, but not between invasive and peritumoral area, and vary between different regions of individual tumors. **a.** Difference between central tumor area and invasive or peritumoral area with regard to vasculature metrics. Microphotographs show representative examples of CD34 staining at x200 magnification in the tumor center (c), at the invasive front (i) and in the peritumoral stroma (s). **b.** Average values of vessel number analyzed with regard to presence of correlation inside one tumor/peritumoral area. Error bars represent average values and 95% CI. Significance of the difference between areas was assessed using Mann–Whitney U test. C, central area; I, invasive front; S, peritumoral stroma.

invasive front was not associated with vessel characteristics of the central tumor area (data not shown).

Together these results suggest a functional relationship between vessel characteristics of the invasive front and GLUT1 expression in cancer cells.

GLUT1 expression and vessel characteristics are correlated with the grade of budding

An additional series of analyses was performed to investigate the associations between budding and the previously described GLUT1 expression and vascular characteristics.

As shown in Table 3, a positive correlation was observed between budding score and GLUT1 expression. The number of buds was also found to be inversely correlated with vessel perimeter at the invasive front and with number of vessels in the peritumoral stroma.

Thus, these data suggest some functional interactions between GLUT1 expression, vasculature and budding at the invasive front, and between budding and vasculature in the peritumoral stroma.

Vasculature metrics, budding and GLUT1 expression are significantly different in tumors with or without lymph node metastasis

Hypoxia, budding and vascular characteristics have been previously reported to be associated with prognosis of CRC. The features described above were therefore analyzed with regard to their association with lymph node metastases.

As shown in Table 4, the vessel perimeter and lumen area of the invasive front were significantly smaller in the group with lymph node metastasis. Also, vessel number in the peritumoral stroma was lower in the lymph node positive group. Finally, in agreement with earlier studies (Saigusa et al., 2012) the lymph node positive group displayed higher budding and GLUT1 expression.

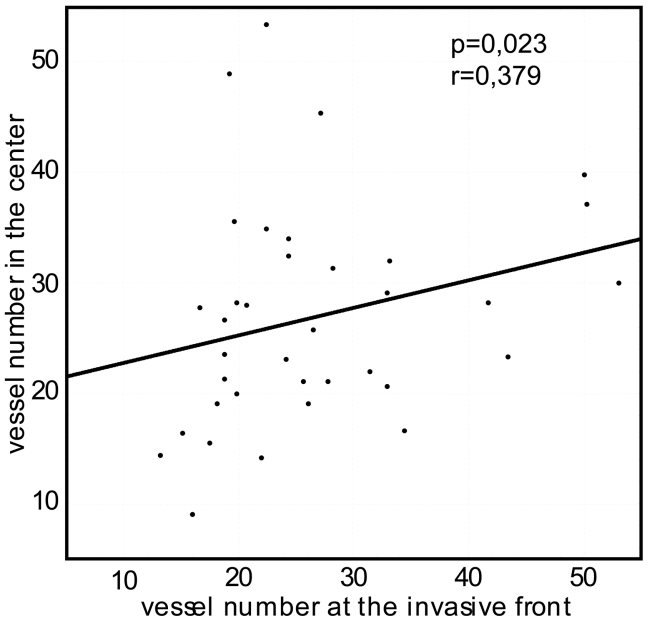

Fig. 2. Vessel number in the central area is correlated to vessel number at the invasive front of the tumor. Mean values of vessel characteristics were analyzed with regard to presence of correlation between different tumor areas. Spearman correlation test was used for analysis.

Table 4. Difference in vessel characteristics, GLUT1 expression and grade of budding in the groups with and without lymph node metastases.

Region and characteristics analyzeda		Lymph node metastases		
		absence	presence	p value
C (n=36)	VN	28.3 (11.0)	26.1 (9.4)	0.397
	VL	7876.1 (4423.2)	6378.2 (1845.6)	0.361
	VP	447.6 (109.4)	399.4 (56.8)	0.281
I (n=39)	VN	23.9 (7.0)	29.5 (11.7)	0.178
	VL	4943.7 (1332.7)	3935.4 (1626.2)	0.006
	VP	351.1 (49.7)	292.6 (18.4)	<0.001
S (n=33)	VN	48.2 (25.2)	29.6 (18.4)	0.014
	VL	4322.0 (1352.9)	5216.9 (4529.7)	0.866
	VP	306.1 (39.9)	309.2 (78.8)	0.721
GLUT1 (n=39)		0.007 (0.013)	0.022 (0.021)	0.001
Budding (n=39)		7.3 (3.5)	12.3 (5.0)	0.001

a, mean values (standard deviations) for vessel characteristics are shown. VN, number of vessels; VL, vessel lumen; VP, vessel perimeter; C, central area; I, invasive front; S, peritumoral fibroblastic stroma; n, number of cases; p, p-value.

Discussion

This is the first study analyzing the interrelation of the expression of GLUT1, vasculature characteristics and budding in colorectal cancer. Vessel characteristics were shown to vary within tumors when central parts, the invasive front and the peritumoral stroma were compared. We observed a previously unreported correlation between GLUT1 expression at the invasive front and vessel characteristics in this area. Also, GLUT1 expression was correlated with the grade of budding.

The general characterization of tumor vasculature demonstrated that the vessels at the invasive area and in the peritumoral region are smaller than vessels in the central part of the tumor. Also, peritumoral vessels are more numerous compared to intratumoral ones. We note that these observations are based on the analyses relying on CD34 antibodies. Previous studies have described that CD31- and CD34-positive vessels represent vasculature of different stages of maturity, with the CD34-postive vessels representing more mature vasculature (Yao et al., 2007). This methodological issue might explain why our findings regarding the variations between the vasculature of the invasive front and the central part of the tumor differ from results obtained in earlier studies using 3D microvascular architecture reconstruction or CD31 staining (Konerding et al., 2001; Vlems et al., 2004).

Interestingly, we detected inter-tumoral variations in vascular metrics when the central part, the invasive part and the peritumoral part are compared in individual tumors (Fig. 1). The implication of this finding is that efforts to link vascular characteristics with prognosis, or response to treatment, need to be relayed on separately collected and analyzed data from these distinct regions.

GLUT1 expression in tumor tissue is generally believed to reflect hypoxia, since GLUT1 expression is largely controlled by hypoxia-inducible factor-1 (HIF-1) (Chen et al., 2001). In this study we analyzed how GLUT1 expression was associated with vascular characteristics of different tumor parts. As shown in Table 2 the strongest observed associations were between high GLUT1 expression and small vessels at the invasive front and high number of vessels at the invasive front. This suggests a functional relationship between GLUT1 status and the vasculature. Another protein regulated by HIF-1 is Vascular Endothelial Growth Factor (VEGF) (reviewed in Quintero et al., 2004). VEGF is an angiogenic factor linked to the extent of neovascularization in CRC (Takahashi et al., 1995). Obviously, the present study cannot establish the direction of causality of this relationship. Possibly, our findings reflect common HIF1-dependent regulation of GLUT1 and VEGF. Future experimental and translational studies should address this.

Our analysis identified a positive correlation between grade of budding and GLUT1 expression. Since GLUT1 is well recognized as a marker of hypoxia these findings largely support earlier studies, which have linked hypoxia to a more invasive and metastatic phenotype (Jang et al., 2012; Hongo et al., 2013).

Another noteworthy finding of the present study is the association between budding and peritumoral vessel density. As shown in Table 3, high budding rate was associated with low number of vessels in the peritumoral area. This finding suggests the presence of functional interaction between tumor invasive border and peritumoral stromal tissue. Future studies should therefore specifically analyze the possible relationships between prognosis and vessel characteristics in non-tumor areas.

The final part of this study explored relationships between lymph node metastasis and the features analyzed in this study. As shown in Table 4, lymph node metastases were positively correlated with four distinct features: high GLUT1 expression, high budding grade, lower vessel number in the peritumoral tissue and smaller vessel size at the invasive front.

Future studies are urged to further explore these issues. Such studies should include larger tumor series, more clinical follow-up information for prognostic analyses, and also aim to investigate specific relationships between cancer cell intrinsic properties,

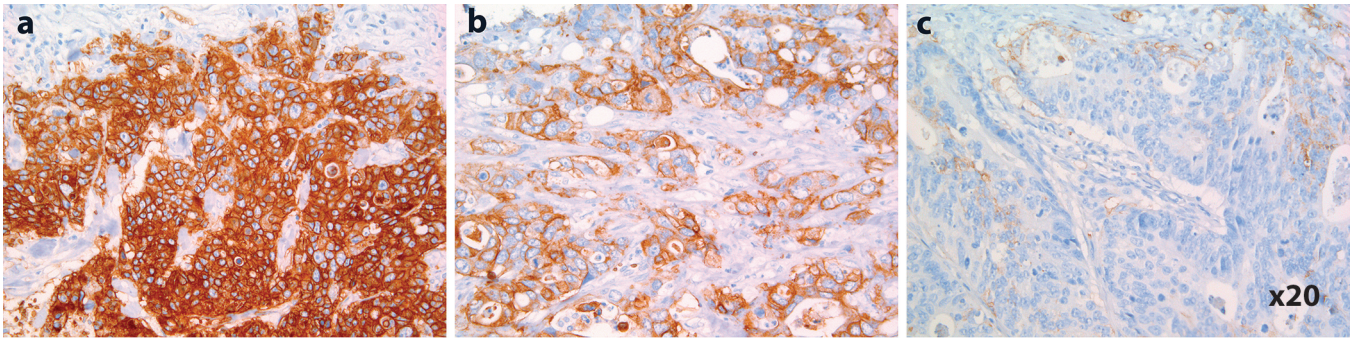

Fig. 3. GLUT1 is variably expressed at the invasive front of CRC. Microphotographs show representative examples of tumors at x200 magnification stained with anti-GLUT1 with high **(a),** medium **(b)** and low **(c)** expression of GLUT1.

such as specific mutations, and vascular features.

Acknowledgements. Degtyarova Marina, MD from Minsk Consulting And Diagnostic Centre, Minsk, Belarus is acknowledged for assisting in immunofluorescence analyses.

CONFLICTS OF INTEREST AND SOURCE OF FUNDING. This work was financially supported by International Science and Technology Center (B-1636). Authors Artur Mezheyeuski (AM), Alexander Nerovnya, Tatjana Bich, Gennadiy Tur and Anna Portyanko have received honoraria from International Science and Technology Center grant B-1636. AM was also supported by a grant from Svenska Institutet.

All authors state no conflicts of interest.

References

Asano T., Katagiri H., Takata K., Lin J.L., Ishihara H., Inukai K., Tsukuda K., Kikuchi M., Hirano H., Yazaki Y. and Oka Y. (1991). The role of N-glycosylation of glut1 for glucose transport activity. J. Biol. Chem. 266, 24632-24636.

Bockhorn M., Jain R.K. and Munn L.L. (2007). Active versus passive mechanisms in metastasis: Do cancer cells crawl into vessels, or are they pushed? Lancet Oncol. 8, 444-448.

Carmeliet P. and Jain R.K. (2011). Molecular mechanisms and clinical applications of angiogenesis. Nature 473, 298-307.

Chen C., Pore N., Behrooz A., Ismail-Beigi F. and Maity A. (2001). Regulation of glut1 mrna by hypoxia-inducible factor-1. Interaction between h-ras and hypoxia. J. Biol. Chem. 276, 9519-9525.

Dachs G.U. and Tozer G.M. (2000). Hypoxia modulated gene expression: Angiogenesis, metastasis and therapeutic exploitation. Eur. J. Cancer 36, 1649-1660.

Ferlay J., Shin H.R., Bray F., Forman D., Mathers C. and Parkin D.M. (2010). Estimates of worldwide burden of cancer in 2008: Globocan 2008. Int. J. Cancer 127, 2893-2917.

Fraisl P., Mazzone M., Schmidt T. and Carmeliet P. (2009). Regulation of angiogenesis by oxygen and metabolism. Dev. Cell 16, 167-179.

Gatenby R.A. and Gillies R.J. (2004). Why do cancers have high aerobic glycolysis? Nat. Rev. Cancer 4, 891-899.

Goh V., Halligan S., Daley F., Wellsted D.M., Guenther T. and Bartram C.I. (2008). Colorectal tumor vascularity: Quantitative assessment with multidetector ct--do tumor perfusion measurements reflect angiogenesis? Radiology 249, 510-517.

Goh V., Rodriguez-Justo M., Engledow A., Shastry M., Endozo R., Peck J., Meagher M., Taylor S.A., Halligan S. and Groves A.M. (2012). Assessment of the metabolic flow phenotype of primary colorectal cancer: Correlations with microvessel density are influenced by the histological scoring method. Eur. Radiol. 22, 1687-1692.

Hongo K., Tsuno N.H., Kawai K., Sasaki K., Kaneko M., Hiyoshi M., Murono K., Tada N., Nirei T., Sunami E., Takahashi K., Nagawa H., Kitayama J. and Watanabe T. (2013). Hypoxia enhances colon cancer migration and invasion through promotion of epithelial-mesenchymal transition. J. Surg. Res. 182, 75-84.

Horcic M., Koelzer V.H., Karamitopoulou E., Terracciano L., Puppa G., Zlobec I. and Lugli A. (2013). Tumor budding score based on 10 high-power fields is a promising basis for a standardized prognostic scoring system in stage ii colorectal cancer. Hum. Pathol. 44, 697-705.

Jang S.M., Han H., Jang K.S., Jun Y.J., Jang S.H., Min K.W., Chung M.S. and Paik S.S. (2012). The glycolytic phenotype is correlated with aggressiveness and poor prognosis in invasive ductal carcinomas. J. Breast Cancer 15, 172-180.

Jass J.R., Barker M., Fraser L., Walsh M.D., Whitehall V.L., Gabrielli B., Young J. and Leggett B.A. (2003). Apc mutation and tumour budding in colorectal cancer. J. Clin. Pathol. 56, 69-73.

Konerding M.A., Fait E. and Gaumann A. (2001). 3d microvascular architecture of pre-cancerous lesions and invasive carcinomas of the colon. Br. J. Cancer 84, 1354-1362.

Krajewska M., Smith L.H., Rong J., Huang X., Hyer M.L., Zeps N., Iacopetta B., Linke S.P., Olson A.H., Reed J.C. and Krajewski S. (2009). Image analysis algorithms for immunohistochemical assessment of cell death events and fibrosis in tissue sections. J. Histochem. Cytochem. 57, 649-663.

Matkowskyj K.A., Cox R., Jensen R.T. and Benya R.V. (2003). Quantitative immunohistochemistry by measuring cumulative signal strength accurately measures receptor number. J. Histochem. Cytochem. 51, 205-214.

Mitrovic B., Schaeffer D.F., Riddell R.H. and Kirsch R. (2012). Tumor budding in colorectal carcinoma: Time to take notice. Mod. Pathol. 25, 1315-1325.

Mosch B., Reissenweber B., Neuber C. and Pietzsch J. (2010). Eph receptors and ephrin ligands: Important players in angiogenesis and tumor angiogenesis. J. Oncol. 2010, 135285.

Portyanko A., Kovalev P., Gorgun J. and Cherstvoy E. (2009). Beta(iii)-tubulin at the invasive margin of colorectal cancer: Possible link to invasion. Virchows Arch. 454, 541-548.

Quintero M., Mackenzie N. and Brennan P.A. (2004). Hypoxia-inducible factor 1 (hif-1) in cancer. Eur. J. Surg. Oncol. 30, 465-468.

Rajaganeshan R., Prasad R., Guillou P.J., Chalmers C.R., Scott N., Sarkar R., Poston G. and Jayne D.G. (2007). The influence of invasive growth pattern and microvessel density on prognosis in colorectal cancer and colorectal liver metastases. Br. J. Cancer 96, 1112-1117.

Rajaganeshan R., Prasad R., Guillou P.J., Scott N., Poston G. and Jayne D.G. (2009). Expression patterns of hypoxic markers at the invasive margin of colorectal cancers and liver metastases. Ejso-Eur. J. Surg. Onc. 35, 1286-1294.

Rizzardi A.E., Johnson A.T., Vogel R.I., Pambuccian S.E., Henriksen J., Skubitz A.P., Metzger G.J. and Schmechel S.C. (2012). Quantitative comparison of immunohistochemical staining measured by digital image analysis versus pathologist visual scoring. Diagn. Pathol. 7, 42.

Ruifrok A.C. and Johnston D.A. (2001). Quantification of histochemical staining by color deconvolution. Anal. Quant. Cytol. Histol. 23, 291-299.

Ruifrok A.C., Katz R.L. and Johnston D.A. (2003). Comparison of quantification of histochemical staining by hue-saturation-intensity (hsi) transformation and color-deconvolution. Appl. Immunohistochem. Mol. Morphol. 11, 85-91.

Saigusa S., Toiyama Y., Tanaka K., Okugawa Y., Fujikawa H., Matsushita K., Uchida K., Inoue Y. and Kusunoki M. (2012). Prognostic significance of glucose transporter-1 (glut1) gene expression in rectal cancer after preoperative chemoradiotherapy. Surg. Today 42, 460-469.

Sullivan R. and Graham C.H. (2007). Hypoxia-driven selection of the metastatic phenotype. Cancer Metastasis Rev. 26, 319-331.

Takahashi Y., Kitadai Y., Bucana C.D., Cleary K.R. and Ellis L.M. (1995). Expression of vascular endothelial growth factor and its

receptor, kdr, correlates with vascularity, metastasis, and proliferation of human colon cancer. Cancer Res. 55, 3964-3968.

Taylor C.R. and Levenson R.M. (2006). Quantification of immunohistochemistry - issues concerning methods, utility and semiquantitative assessment ii. Histopathology 49, 411-424.

Vlems F., van der Worp E., van der Laak J., van de Velde C., Nagtegaal I. and van Krieken H. (2004). A study into methodology and application of quantification of tumour vasculature in rectal cancer. Virchows Arch. 445, 263-270.

Yao X., Qian C.N., Zhang Z.F., Tan M.H., Kort E.J., Yang X.J., Resau J.H. and Teh B.T. (2007). Two distinct types of blood vessels in clear cell renal cell carcinoma have contrasting prognostic implications. Clin Cancer Res. 13, 161-169.

Zhang S.C., Hayashi R., Fujii M., Hasegawa Y., Yoshino K., Fukayama M. and Ochiai A. (2009). Total microvessel perimeter per tumor area is a predictor of radiosensitivity in early-stage glottic carcinoma. Int J. Radiat. Oncol. 73, 1104-1109.

Accepted March 26, 2015